Communication

Solution Structure of HIV-1 Protease Flaps Probed by Comparison of Molecular Dynamics Simulation Ensembles and EPR Experiments

Fangyu Ding, Melinda Layten, and Carlos Simmerling

J. Am. Chem. Soc., **2008**, 130 (23), 7184-7185 • DOI: 10.1021/ja800893d • Publication Date (Web): 15 May 2008

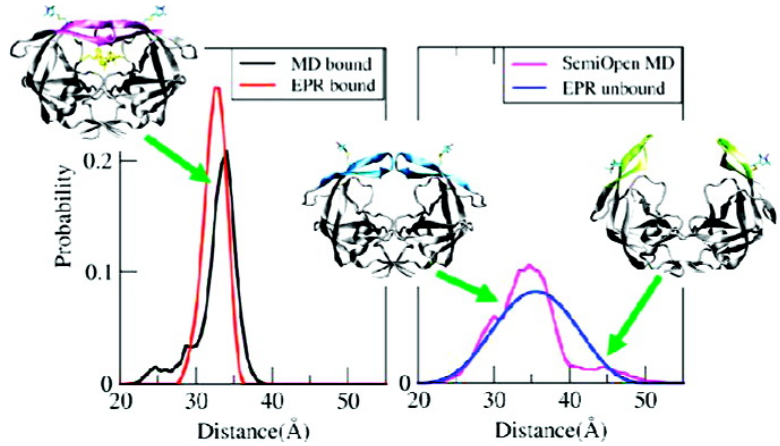

More About This Article

Additional resources and features associated with this article are available within the HTML version:

- Supporting Information
- Links to the 5 articles that cite this article, as of the time of this article download
- Access to high resolution figures
- Links to articles and content related to this article
- Copyright permission to reproduce figures and/or text from this article

View the Full Text HTML

J|A|C|S
COMMUNICATIONS

Published on Web 05/15/2008

Solution Structure of HIV-1 Protease Flaps Probed by Comparison of Molecular Dynamics Simulation Ensembles and EPR Experiments

Fangyu Ding,[†] Melinda Layten,[‡] and Carlos Simmerling*[,†,‡]

Department of Chemistry and Graduate Program in Molecular and Cellular Biology, Stony Brook University, Stony Brook, New York 11794

Received February 4, 2008; E-mail: carlos.simmerling@stonybrook.edu

The introduction of multidrug treatment has dramatically prolonged the progression and survival of AIDS patients. However, the success of long-term treatment has been hindered by strains of HIV that are increasingly resistant to inhibitors of targets such as HIV protease (HIV PR).[1] Therefore, the need for a thorough understanding of the structure and dynamics of HIV PR and how these are altered in resistant mutants is crucial for the design of more effective treatments.[2] Crystal structures of unbound HIV PR show significant heterogeneity and often have extensive crystal packing interactions. In this report, we link EPR experiments and MD simulations to gain insight into the ensemble of HIV PR conformations sampled in solution, both in the presence and in the absence of an FDA-approved HIV PR inhibitor. We find that the trends in the spin label distance distributions obtained from EPR data for bound and unbound HIV PR are only reproduced by a simulation model in which the protease significantly changes conformation upon binding. Furthermore, the longest spin label distances are only sampled by fully open HIV PR structures transiently observed during MD.

At present, diverse techniques have provided valuable structural information about HIV PR, including X-ray crystallography, nuclear magnetic resonance (NMR), electron paramagnetic resonance (EPR), and molecular dynamics (MD) simulations. Crystal structures of all ligand-bound proteases are homogeneous,[3,4] showing the two flexible glycine-rich β-hairpins, the so-called "flaps", interacting with the ligand and completely blocking access to the active site (Figure 1a). In contrast, crystal structures of the ligand-free protease reported to date are more heterogeneous;[5] nearly all exhibit the "semiopen" form (Figure 1b), although "closed" and "wide-open" forms have also been reported. Interestingly, active site access remains blocked in both the closed and semiopen forms, thus large-scale flap opening is presumably required to allow substrate entry. However, we recently demonstrated[6] that the crystallographic wide-open structure[7] may be an artifact of the extensive interactions between symmetry-related neighbors. Furthermore, this crystal structure differs substantially from the transient open form we observed in our previous[8] and the present study (Figure 1c). Earlier studies also suggested a role for crystal packing in the semiopen form.[9−11] Other calculations have suggested that the free energy difference between the semiopen and closed conformations may be quite small,[12] implying that the equilibrium of different configurations of the flaps might be easily shifted by many factors such as mutations, ligand binding, and even crystal contacts.

Although the relationship between the apparent conformational flexibility and catalytic activity is still unclear, it has been suggested that resistance mutations might affect the flexibility of the unbound enzyme. For example, M46I appears to stabilize the closed form of the flaps.[13] To date, obtaining structural data on the ensemble of structures adopted by the flaps in solution is not readily accessible to experiment. Solution NMR experiments on unbound HIV PR indicate that the flap tips experience rapid (nanoseconds) local fluctuations, while larger motions of the entire flaps occur on the microsecond time scale.[14] Recently, Fanucci's laboratory performed site-directed spin labeling (SDSL) to probe conformational flexibility of the flaps in the absence and presence of an inhibitor (Ritonavir), via double electron−electron resonance (DEER) spectroscopy for unpaired nitroxide electrons in labels attached to K55C/K55′C on the HIV PR flaps.[15] This work is particularly notable since it revealed a markedly different extent of label flexibility in the bound and unbound forms, with an interspin distance distribution that is narrower and has a shorter average in the inhibitor-bound as compared to unbound protease.

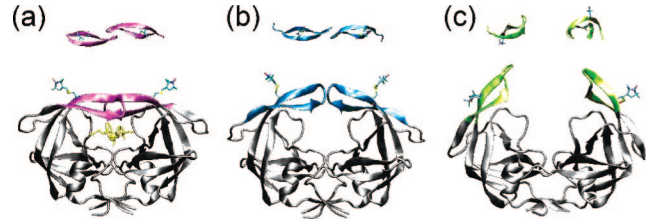

Figure 1. Three conformations of HIV PR during all-atom MD with EPR spin labels: (a) closed Ritonavir bound, (b) semiopen unbound, (c) fully open unbound. Top views illustrate the reversal of handedness between the closed and semiopen form and the separation of open flaps.

The distance measured by SDSL is based on the dipolar coupling between two unpaired nitroxide electrons, which are located ~7 Å from the C_α atom of the protein backbone (Figure 1). Thus the information obtained from this technique reports only indirectly on the behavior of the flaps themselves. It is likely that the observed label distributions report on flap dynamics, rather than changes in the label as a result of inhibitor binding. The shift in distribution in the presence of inhibitor could reflect the rearrangement of the flaps from semiopen to closed handedness (Figure 1a,b top) or could arise from decreased flap motion due to direct interactions between flaps and inhibitor (Figure 1a). However, the successful interpretation of SDSL-EPR data and potential application to drug-resistant HIV PR requires additional data concerning which specific flap conformations give rise to particular ranges of spin label distances, and how these ensembles are affected by inhibitor binding. Importantly, it is unclear whether the observed interspin distance distribution can be explained solely by an ensemble consisting of conformations seen in the various crystal structures. Therefore, establishing a correlation between EPR-measured interspin distances and structural dynamic features of the flaps is essential in the interpretation of the current and future EPR data for this system.

[†] Department of Chemistry.
[‡] Graduate Program in Molecular and Cellular Biology.

10.1021/ja800893d CCC: $40.75

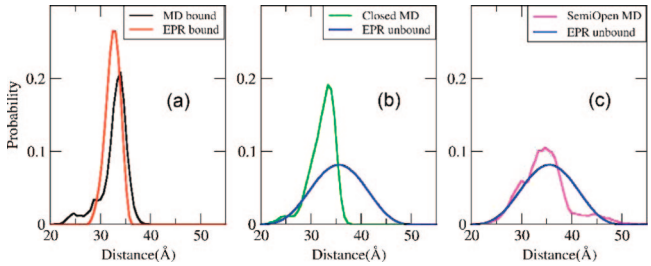

Figure 2. MTSL spin label distances from experiment and MD. Simulations of bound closed (a); unbound closed (b); unbound semiopen (c). The same unbound EPR-based data are shown in (b) and (c).

We have previously shown that our simulation model of HIV PR is able to accurately reproduce a spontaneous change between semiopen and closed handedness upon addition or removal of a cyclic urea inhibitor.[8,16] We employed this model, with addition of spin label probes[17] to the simulated HIV PR, for comparison against EPR-based data in order to determine the ensemble of conformations that best agrees with EPR data.

We performed a series of MD simulations, in fully explicit solvent with the ff99SB protein force field,[18] using the LAI consensus HIV PR sequence (with several mutations to match the EPR experiment, see Supporting Information) and methanethiosulfonate (MTSL) spin labels attached via disulfide bonds at C55 and C55′. Bound HIV PR simulations used closed coordinates. Simulations for unbound protease were initiated from both semiopen and closed coordinates. Two simulations of 150 ns were performed for each of the three systems (750 ns total).

In the Ritonavir-bound simulations, the MTSL N−N distance was confined to 30−33 Å, in near-quantitative agreement with EPR measurement of the bound HIV PR (Figure 2a), and reflects a restricted amplitude of flap motions, perhaps due to the flap−inhibitor interaction. However, in the unbound closed simulations, the N−N distance exhibited similar restricted fluctuations as in Ritonavir-bound simulations (Figure 2b), with a similar average distance despite loss of flap−inhibitor interactions. This unbound closed model is in disagreement with the EPR data, suggesting that simple loss of the inhibitor is not enough to account for the observed trends in both width and average of the nitroxide distance distribution. Intraflap hydrogen bonding was observed in these simulations, contributing to the stability of the closed flaps on the >100 ns time scale of our simulations (see Supporting Information). This observation is consistent with the microsecond time scale of large-scale flap motion suggested by NMR,[14] further indicating that nanosecond time scale flap tip motion is not responsible for the changes seen in the EPR data upon inhibitor binding.

In unbound semiopen simulations, significant but transient opening and closing events were observed, giving further evidence for the considerable variability of this flap configuration. A significantly longer and wider N−N distance distribution was obtained, in very good agreement with EPR measurements of unbound HIV PR (Figure 2c). We note that spin label side chain motion also contributes to the distribution since structures with flap backbone rmsd values of <1 Å still span a range of distances from 30 to 40 Å (Figure S2).

Importantly, MD structures with label distances greater than 40 Å always had flap rmsd values of at least 3 Å as compared to the closed, semiopen, and wide-open crystallographic forms (see Supporting Information). This suggests that the EPR-based ensemble includes flap conformations that match *none* of the reported unbound crystal structures but can indeed be explained by full opening events as observed in MD. Nonetheless, a discrepancy in the distance distribution between MD simulations and EPR measurement remains; structures with long nitroxide distances (40−45 Å) are present in the simulations but at a lower population than indicated by EPR data. The difference cannot be explained solely by changes in equilibrium among the crystal forms since none of those structures can sample long enough distances. A likely source of uncertainty is that, even with >100 ns of simulation, the MD population of fully open structures has not reached convergence. Furthermore, the simulations modeled only the dimer, while the experiment likely also contains a population of monomeric HIV PR. It will also be important to determine whether the contribution of these "open" structures with long label distances changes as the glassing agents used in the EPR experiments are varied.

Overall, the N−N distances sampled in semiopen unbound simulations are in much better agreement with the EPR data than are the simulations initiated with the closed HIV PR structure, suggesting that the semiopen form is the dominant configuration for this ligand-free HIV PR in solution, at least under the conditions probed by EPR. These data strongly support the hypothesis that the flaps in the unbound state exist in a diverse ensemble of conformations fluctuating between semiopen, closed, and open, exhibiting considerable flexibility to allow substrate entry and product exit.

Acknowledgment. We thank Luis Galiano and Gail Fanucci for helpful discussions, Ian Haworth for MTSL parameters, and the NIH (GM6167803) and NCSA (NPACI MCA02N028).

Supporting Information Available: Detailed methods, parameters, and additional analyses. This material is available free of charge via the Internet at http://pubs.acs.org.

References

(1) Walensky, R.; Paltiel, A. D.; Losina, E.; Mercincavage, L.; Schackman, B.; Sax, P.; Weinstein, M.; Freedberg, K. *J. Infect. Dis.* **2006**, *194* (1), 11–19.
(2) Hornak, V.; Simmerling, C. *Drug Discovery Today* **2007**, *12* (3−4), 132–138.
(3) Wlodawer, A.; Miller, M.; Jaskolski, M.; Sathyanarayana, B. K.; Baldwin, E.; Weber, I. T.; Selk, L. M.; Clawson, L.; Schneider, J.; Kent, S. B. H. *Science* **1989**, *245* (4918), 616–621.
(4) Zoete, V.; Michielin, O.; Karplus, M. *J. Mol. Biol.* **2002**, *315* (1), 21–52.
(5) Vondrasek, J.; Wlodawer, A. *Proteins: Struct., Funct., Genet.* **2002**, *49* (4), 429–431.
(6) Layten, M.; Hornak, V.; Simmerling, C. *J. Am. Chem. Soc.* **2006**, *128* (41), 13360–13361.
(7) Martin, P.; Vickrey, J. F.; Proteasa, G.; Jimenez, Y. L.; Wawrzak, Z.; Winters, M. A.; Merigan, T. C.; Kovari, L. C. *Structure* **2005**, *13* (12), 1887–1895.
(8) Hornak, V.; Okur, A.; Rizzo, R. C.; Simmerling, C. *J. Am. Chem. Soc.* **2006**, *128* (9), 2812–2813.
(9) Lange-Savage, G.; Berchtold, H.; Liesum, A.; Budt, K. H.; Peyman, A.; Knolle, J.; Sedlacek, J.; Fabry, M.; Hilgenfeld, R. *Eur. J. Biochem.* **1997**, *248* (2), 313–322.
(10) Harte, W. E., Jr.; Swaminathan, S.; Mansuri, M. M.; Martin, J. C.; Rosenberg, I. E.; Beveridge, D. L. *Proc. Natl. Acad. Sci. U.S.A.* **1990**, *87* (22), 8864–8868.
(11) York, D. M.; Darden, T. A.; Pedersen, L. G.; Anderson, M. W. *Biochemistry* **1993**, *32* (12), 3196–3196.
(12) Rick, S. W.; Erickson, J. W.; Burt, S. K. *Proteins: Struct., Funct., Bioinf.* **1998**, *32* (1), 7–16.
(13) Collins, J. R.; Burt, S. K.; Erickson, J. W. *Nat. Struct. Mol. Biol.* **1995**, *2* (4), 334–338.
(14) Ishima, R.; Freedberg, D. I.; Wang, Y. X.; Louis, J. M.; Torchia, D. A. *Structure* **1999**, *7* (9), 1047–1055.
(15) Galiano, L.; Bonora, M.; Fanucci, G. E. *J. Am. Chem. Soc.* **2007**, *129* (36), 11004–11005.
(16) Hornak, V.; Okur, A.; Rizzo, R. C.; Simmerling, C. *Proc. Natl. Acad. Sci. U.S.A.* **2006**, *103* (4), 915–920.
(17) Price, E. A.; Sutch, B. T.; Cai, Q.; Qin, P. Z.; Haworth, I. S. *Biopolymers* **2007**, *87* (1), 40–50.
(18) Hornak, V.; Abel, R.; Okur, A.; Strockbine, B.; Roitberg, A.; Simmerling, C. *Proteins: Struct., Funct., Bioinf.* **2006**, *65* (3), 712–725.

JA800893D